ISOMAse
International Society of Ocean, Mechanical and Aerospace Scientists and Engineers

Journal of Ocean, Mechanical and Aerospace
-Science and Engineering-
30th March 2024. Vol.68 No.1

March 30, 2024

Investigation of the Effect of CFRP and GFRP Sheet Length on the Final Capacity of Reinforced Concrete Beams of Buildings in Coastal Areas

Ali Rasoulian Mashhadi,[a] Hamid Varastehpour,[b] and Seyed-Mahmood Ghassemizadeh,[c*]

[a)] *MSc Graduate, Department of Civil Engineering, Islamic Azad University (Science and Research), Neyshabour, Iran*
[b)] *Assistant Professor, Higher Education Complex Utilities Industry in Khorasan, Mashhad, Iran*
[c)] *MSc Graduate, Department of Maritime Engineering, Amirkabir University of Technology, Tehran, Iran*

*Corresponding author: ghassemizadeh@aut.ac.ir

Paper History

Received: 02-December-2023
Received in revised form: 10-January-2024
Accepted: 30-March-2024

ABSTRACT

In the last two decades, the use of FRP (Fiber Reinforced Polymer) composites for flexural, shear, torsion, and enclosing reinforcement of various structural components has grown exponentially. In this paper, the effect of using FRP composite with carbon fibers and glass with different lengths on the behavior of reinforced concrete beams is investigated. Eight reinforced concrete beams with a length of 150 cm, a width of 15 cm, and a height of 20 centimeters were modeled by composite fibers with lengths of 80 cm, 100 cm, 120 cm and 140 centimeters. Then, the sample reinforced concrete beam was modeled in ABAQUS®, which the results were compared with the laboratory samples. It were observed that with increasing the length of FRP sheets, the strength of reinforced concrete beams compared to the sample concrete beam, increased by about 61%, 82%, 86%, and 87%, respectively. It was due to the high cost of FRP sheets and compressive strength required in these sheets that used optimally. Therefore, the length of FRP strengthening sheets can be optimized to reduce the cost of FRP sheets and use them efficiently.

KEYWORDS: *Reinforced concrete beam, Strengthening, CFRP sheet, GFRP sheet, ABAQUS®, Laboratory study.*

NOMENCLATURE

FEM	Finite Element Method
EXP	Experimental Method
FRP	Fiber Reinforced Polymer
CFRP	Carbon Fiber Reinforced Polymer
GFRP	Glass Fiber Reinforced Polymer

1.0 INTRODUCTION

In recent years, the retrofitting of existing structures has become increasingly important. Various reasons contribute to this, such as the aging of structures and an increase in design and construction errors. Additionally, many existing structures, due to increased applied loads, require reinforcement [1]. From both, environmental and economic perspectives, retrofitting, repair, strengthening, and upgrading of existing structures are prioritized over the demolition and reconstruction of structures. Moreover, in many cases, retrofitting is more cost-effective and less troublesome than rebuilding. Furthermore, the speed of retrofitting is often faster than reconstruction, preventing structures from being out of service for extended periods [2] and [3].

One of the recent advancements in retrofitting is the use of Fiber Reinforced Polymer (FRP) composite overlays, which are employed to strengthen concrete, steel, masonry, and even wooden structures. The initial research on FRP fibers dates back to the early 1980s, but the earthquakes in 1990 in California and 1995 in Kobe, Japan, played a crucial role in comprehensively investigating the application of polymer composites made of FRP fibers for the reinforcement and retrofitting of concrete and masonry structures in earthquake-prone areas. Currently, numerous researchers and structural engineering professionals worldwide are studying, researching, and conducting experiments on structure strengthening using FRP composites [4]-[6]. Mostofinejad & Hajrasouliha (2009) investigated the effect of the depth and width of longitudinal grooves, as well as the compressive strength of samples, to prevent premature debonding in unreinforced and CFRP-reinforced concrete samples [7]. Mestofinanjad & Mahmoudabadi (2010) proposed a new method of slotting as a suitable approach to prevent early failure, demonstrating that changing the groove type from transverse to circular and ultimately longitudinal increases the ultimate load capacity [8]. Mestofinanjad & Shamlou (2010) conducted experiments on unreinforced concrete beams strengthened with 1, 2, and 3 layers of CFRP using surface preparation, slotting, and surface bonding methods, examining the effectiveness of each method

ISOMAse International Society of Ocean, Mechanical and Aerospace Scientists and Engineers

Journal of Ocean, Mechanical and Aerospace
-Science and Engineering-
30th March 2024. Vol.68 No.1

March 30, 2024

[9]. Sadrmamtaz & Rostami-Attieh (2012) subjected 9 concrete beams, 8 of which were reinforced with a single layer of CFRP, to flexural testing. They demonstrated an increase in load-bearing capacity by 26% and 32% and an increase in ductility by 77% and 90% [10].

Varastehpour & Eskandari (2015) investigated samples of GFRP-strengthened concrete beams where premature debonding, concrete cover cracking, and separation of the concrete and the reinforcing plate occurred [11]. Varastehpour & Kermani (2015) presented a combined method using classic and L-shaped bonding for CFRP plates to increase the concrete section capacity, showing a 10% and 40% increase in flexural strength without reinforcement compared to other methods [12]. Arefian & Mestofinanjad (2015) [13] evaluated the effective anchorage length of FRP strengthening plates using the external bonding technique on concrete surfaces with compressive strength less than 30 MPa, between 30 and 40 MPa, and above 40 MPa. They found the demonstrating result that increasing the length of the external FRP plate connection to concrete cannot guarantee full tensile strength [13]. Mozinani et al. (2015) compared the use of multiple layers of high-strength GFRP with multiple layers of high-strength CFRP in terms of ductility, showing that the use of multiple layers of GFRP increased ductility compared to multiple layers of CFRP [14].

This article discusses experimental and numerical investigations into the effect of the length of FRP (Fiber Reinforced Polymer) plates, specifically CFRP (Carbon Fiber Reinforced Polymer) and GFRP (Glass Fiber Reinforced Polymer), on the ultimate capacity of reinforced concrete beams. In this regard, eight specimens of reinforced concrete beams with dimensions of 1,500 mm length, 150 mm width, and 200 mm height were subjected to four-point bending tests. The experimental and theoretical results were analyzed using ABAQUS® software.

2.0 METHOD

The FRP (Fiber Reinforced Polymer) sheets are among the construction materials composed of two or more constituent materials that work together cohesively. Research conducted in recent years has proven that fiber-reinforced polymers in repair and reconstruction of structures are more efficient and beneficial than other methods, addressing many challenges related to the strengthening of concrete and steel structures. However, concerns exist regarding some effects that may impact the properties of FRP materials and the bond between concrete and FRP sheets, with premature debonding being a notable concern. One of the significant reasons for premature debonding is the unpreparedness of the concrete surface for proper bonding with the FRP sheet. Overall, it can be said that FRP fibers have very high tensile strength, and their stress-strain behavior is linear until failure. This behavior comes with two major drawbacks:

1. Members reinforced with fibers have less ductility. However, in cases where confinement is required (such as in columns), they increase both resistance and ductility.
2. The distribution of stresses is limited due to the lack of ductility.

It can be seen in Table 1, the comparison of performance characteristics of carbon, glass, and aramid composites in concrete beams. In this experiment, eight specimens of reinforced concrete beams with dimensions of 1500 mm x 150 mm x 200 mm, were prepared in metal molds. Each beam was reinforced with two longitudinal grade 10 rebars of type AIII at the bottom of the section, grade 8 stirrups of type AII spaced 10 cm apart, and a grade 6 longitudinal rebar without stirrup of type AI at the top of the section to maintain spacing between the stirrups. The arrangement is illustrated in Figures 1 and 2.

Table 1: Performance comparison of carbon, glass, and aramid composites in reinforcing beams

Aramid Composite	Glass Composite	Carbon Composite	Usage in Beam Reinforcement
Good	Adequate	Very Good	Flexural (Bending)
Good	Inadequate	Very Good	Shear
Inadequate	Inadequate	Very Good	Serviceability

Figure 1: Layout/configuration of concrete beams

Figure 2: Reinforcement of concrete beams

ISOMAse
International Society of Ocean, Mechanical and Aerospace Scientists and Engineers
Journal of Ocean, Mechanical and Aerospace
-Science and Engineering-
30th March 2024. Vol.68 No.1

Figure 3: The concrete pouring operations in 8 samples

Figure 4: The cubic samples for determining concrete compressive strength

Six cubic samples with dimensions of 150x150x150 mm were taken for the purpose of measuring the 28-day compressive strength. Two samples were obtained from each concrete pouring series, as illustrated in Figures 3 and 4. To achieve a 28-day compressive strength of 30 MPa in the concrete used in the specimens, the guidelines outlined in the ACI 211.1-91 standard were followed. The results of the fractured samples are presented in Table 2. Additionally, to control the quality and determine the materials, ASTM C33/C33M-18 standard procedures were followed, as shown in Table 3. The fibers used in this research are of CFRP and GFRP types, and their specifications are provided in Table 4. The adhesives, or polymer resins, play the role of transferring forces between fibers and concrete and serve as a holding material for CFRP and GFRP fibers. The specifications of the two-part epoxy resin used in this research are presented in Table 5. The resin-to-hardener ratio in this study is considered as 1 to 0.58. Each of these samples (beams) is labeled with titles B0, B1, B2, B3, B4, B5, B6, and B7. Samples B4 and B7 were analyzed using ABAQUS® software. The specifications of all models are presented in Table 6.

A thin and uniform layer of adhesive was first applied to the concrete surface, and then the fibers were placed on it, to adhere the fiber layers to the samples. For bonding the fibers to the desired surface using a trowel, the adhesive was again completely and uniformly applied to ensure complete adhesion. Subsequent layers were adhered in the same manner. Finally, a uniform layer of adhesive was applied to the soaked fibers to protect them, completing the connection between the fibers. After completing these steps, the samples were stored for seven days and prepared for loading. The preparation process is illustrated in Figures 5.

Table 2: Compressive Strength of the Concrete Used in Beam Construction

Sample Number	Strength Mpa
1	27
2	29
3	30
4	30
5	32
6	31

Table 3: Specifications of the Concrete Used in Beam Construction

Type of Material	Consumption kg/m³
Water	200
Cement	400
Gravel	700
Sand	1050

Table 4: Physical Specifications of CFRP and GFRP Composite Sheets Used

Fiber Material	Ultimate Tensile Strength MPa	Modulus of Elasticity GPa	Thickness mm
Carbon Fiber	4900	230	0.111
Glass Fiber	2300	76	0.16

Table 5: Physical Specifications of the Used Resin

Tensile Strength MPa	Tensile Modulus MPa	Flexural Modulus GPa
30	2500	2700

Figure 5: Performing preparation operations and adhering FRP sheets to the samples

JOMAse | Received: 02-December-2023 | Accepted: 30-March-2024 | [(68) 1: 1-8]
Published by International Society of Ocean, Mechanical and Aerospace Scientists and Engineers, www.isomase.org., ISSN: 2354-7065 & e-ISSN: 2527-6085

Journal of Ocean, Mechanical and Aerospace
-Science and Engineering-
30th March 2024. Vol.68 No.1

Table 6: Specifications of prepared surfaces of the constructed beam samples

Row	Sample Name	Type of Surface Preparation	Type and Number of Reinforcement Sheets	Description of the Sample
1	B_0	No	---	Control Sample - Does not have any reinforcing sheets
2	B_1	Angle grinder with Special Stone	2 Layers CFRP	A CFRP sheet with a length of 80 cm across the entire width of the beam
3	B_2	Angle grinder with Special Stone	2 Layers CFRP	A CFRP sheet with a length of 100 cm across the entire width of the beam
4	B_3	Angle grinder with Special Stone	2 Layers CFRP	A CFRP sheet with a length of 120 cm across the entire width of the beam
5	B_4	Angle grinder with Special Stone	2 Layers CFRP	A CFRP sheet with a length of 140 cm across the entire width of the beam
6	B_5	Angle grinder with Special Stone	2 Layers GFRP	A GFRP sheet with a length of 80 cm across the entire width of the beam
7	B_6	Angle grinder with Special Stone	2 Layers GFRP	A GFRP sheet with a length of 100 cm across the entire width of the beam
8	B_7	Angle grinder with Special Stone	2 Layers GFRP	A GFRP sheet with a length of 120 cm across the entire width of the beam
9	B_8	Angle grinder with Special Stone	2 Layers GFRP	A GFRP sheet with a length of 140 cm across the entire width of the beam

3.0 RESULTS AND DISCUSSION

3.1 Description of Modeling and Laboratory Procedures

For the experiments, all beams were placed as simply supported and subjected to four-point bending loading. Loading was controlled with a rate of 10 kilograms per second, and the load-deformation diagram was recorded using a 200-ton jack. Beam B0 (Figure 6) was without external reinforcement, served as the control beam for comparison with other beams. After applying the load, it failed due to flexural cracks in the center of the beam. Beam B1 (Figure 7), with two layers of CFRP across the width of the beam, 80 centimeters long from the center to the supports, experienced flexural and shear cracks in the tension zone before reaching its maximum bending capacity and eventually collapsed. Beam B2 (Figure 8), with two layers of CFRP across the width of the beam, 100 centimeters long from the center to the supports, suffered premature deboning and delamination of CFRP sheets in the tension zone, causing the concrete cover to spall before reaching its maximum flexural capacity. Beam B3 (Figure 9), with two layers of CFRP across the width of the beam, 120 centimeters long from the center to the supports, failed due to cracks in the tension zone and shear failure before reaching its maximum bending capacity.

Beam B4 (Figure 10), reinforced with two layers of CFRP across the width of the beam with a length of 140 centimeters from the center to the supports, after loading, experienced cracking in the flexural loading area. After reaching the maximum flexural capacity, it suffered early cracking, followed by fragmentation of the compressive concrete in the tensile area, and subsequently collapsed. Beam B5 (Figure 11) is reinforced with two layers of GFRP. This beams, before reaching the maximum flexural capacity, experienced cracking in the flexural loading area due to flexural and shear cracks, leading to its collapse. Beam B6 (Figure12) is reinforced with two layers of GFRP. This beam, before reaching the maximum flexural capacity, collapsed due to shear failure in the tensile area of the concrete from the loading point to the support.

Beam B7 (Figure 13) is reinforced with two layers of GFRP. This beam, before reaching the maximum flexural capacity, collapsed due to the delamination of the GFRP sheets in the tensile area of the concrete and shear failure from the loading point to the support. Beam B8 (Figure 14) is reinforced with two layers of GFRP. This beam, before reaching the maximum flexural capacity, collapsed due to the delamination of the GFRP sheets in the tensile area of the concrete and shear failure (shear cracking) from the loading point to the support.

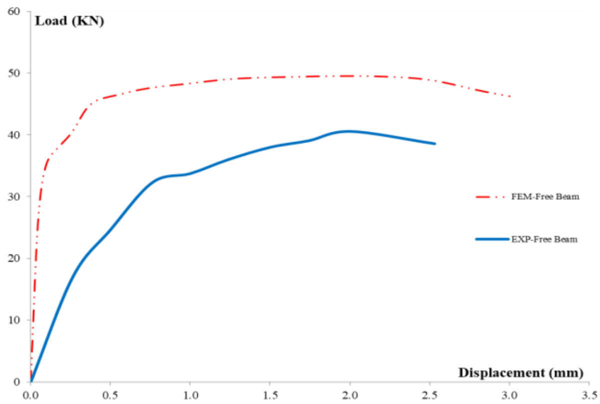

Figure 6: Beam B0 after loading operations

JOMAse | Received: 02-December-2023 | Accepted: 30-March-2024 | [(68) 1: 1-8]
Published by International Society of Ocean, Mechanical and Aerospace Scientists and Engineers, www.isomase.org., ISSN: 2354-7065 & e-ISSN: 2527-6085

ISOMAse
International Society of Ocean, Mechanical and Aerospace Scientists and Engineers

Journal of Ocean, Mechanical and Aerospace
-Science and Engineering-
30th March 2024. Vol.68 No.1

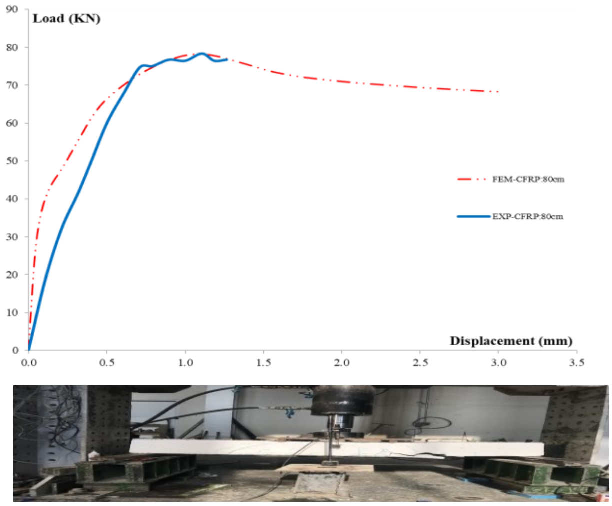

Figure 7: Beam B1 after loading operations

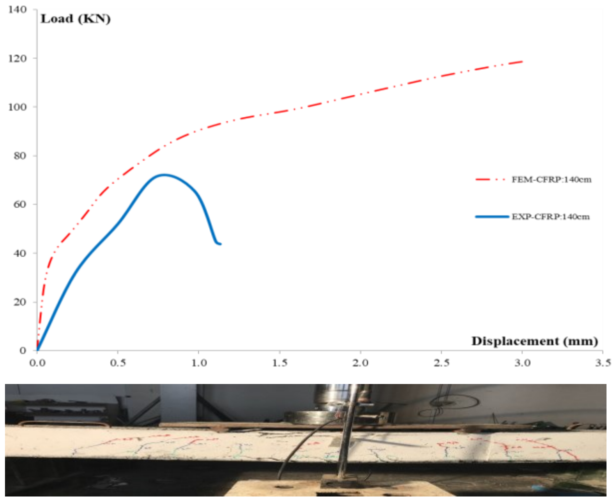

Figure 10: Beam B4 after loading operations

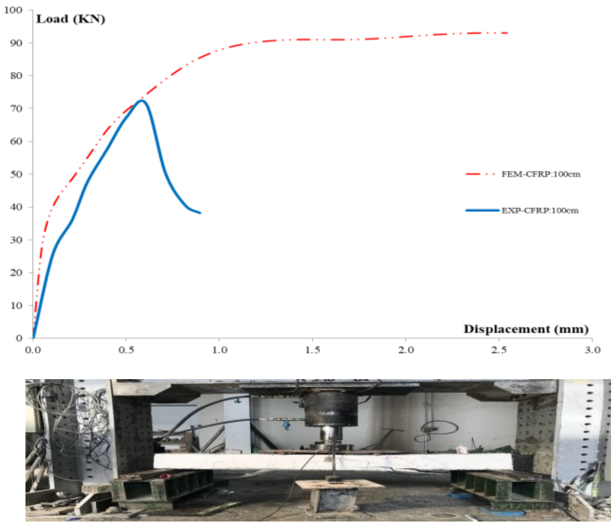

Figure 8: Beam B2 after loading operations

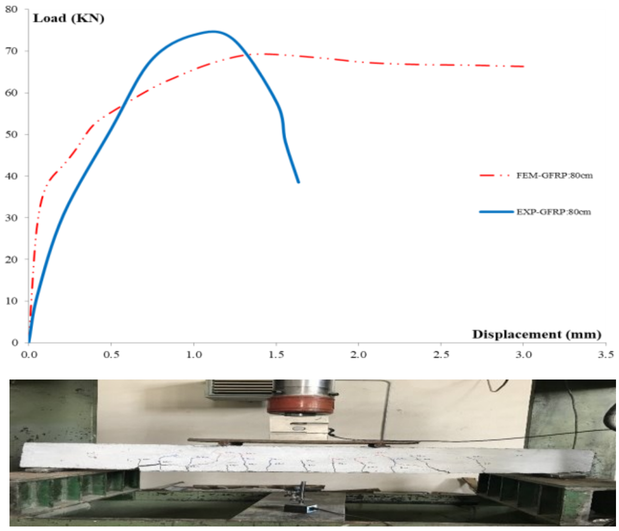

Figure 11: Beam B5 after loading operations

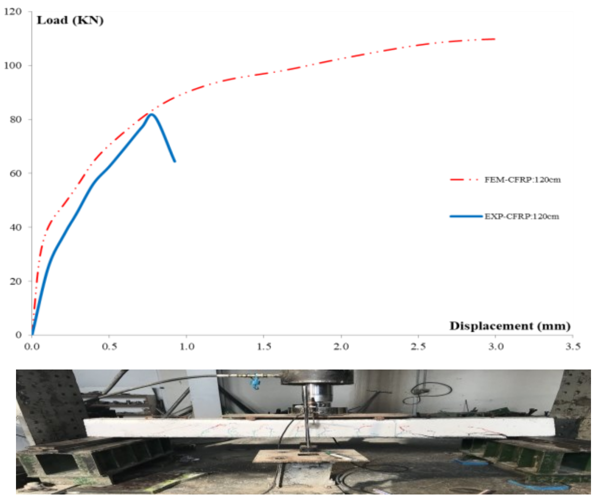

Figure 9: Beam B3 after loading operations

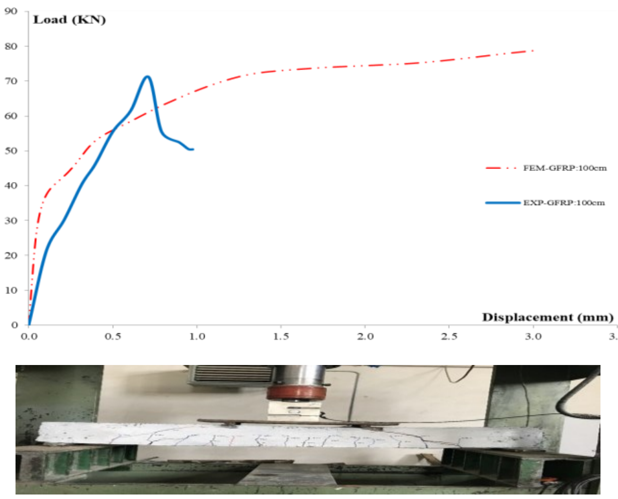

Figure 12: Beam B6 after loading operations

JOMAse | Received: 02-December-2023 | Accepted: 30-March-2024 | [(68) 1: 1-8]
Published by International Society of Ocean, Mechanical and Aerospace Scientists and Engineers, www.isomase.org., ISSN: 2354-7065 & e-ISSN: 2527-6085

ISOMAse
International Society of Ocean, Mechanical and Aerospace Scientists and Engineers

Journal of Ocean, Mechanical and Aerospace
-Science and Engineering-
30th March 2024. Vol.68 No.1

March 30, 2024

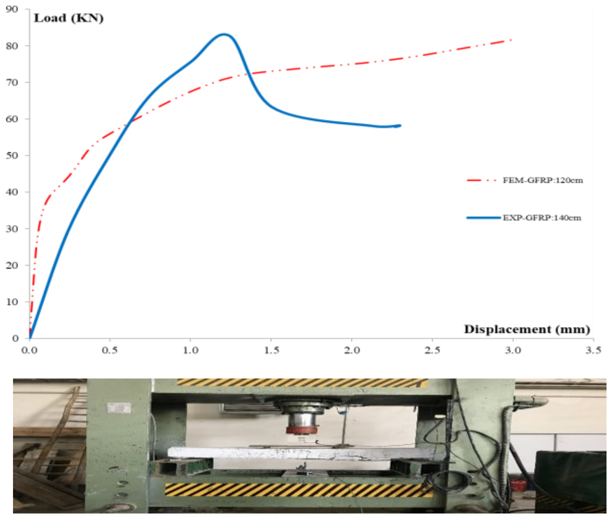

Figure 13: Beam B7 after loading Operations

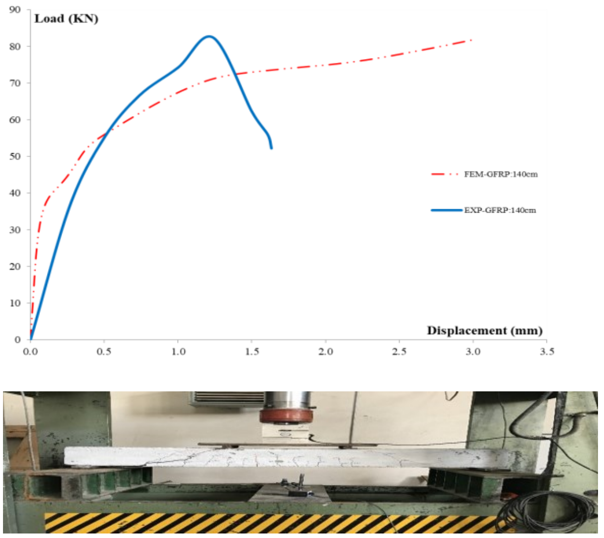

Figure 14: Beam B8 after loading operations

3.2 Interpretation of Experimental Results

The results of resistances and displacements of the tested beams are presented in Table 7. As observed, the use of various FRP sheets for reinforcement has been highly beneficial, but due to the phenomenon of premature failure, the section capacity exceeds the experimental value. In this table, the theoretical section capacity results are also compared. The load-deformation behavior of beams with carbon and glass fibers is shown in Figures 15 and 16, respectively. It is observed that with the increase in the length of carbon and glass sheets, the flexural capacity increases, and the deflection at ultimate resistance relatively decreases. The comparison of all modeled specimens in the ABAQUS® is shown in Figure 17. As indicated in Table 8, beams B1, B2, B3, and B4 have been reinforced at a lower cost (lower consumption of carbon fibers and adhesive) and, accordingly, have lower ultimate resistances. This pattern is also true for beams B5, B6, B7, and B8, reinforced with glass fibers. Therefore, the choice of the length and type of FRP sheets depends on the specific conditions of the structure and the design preferences regarding the mentioned advantages.

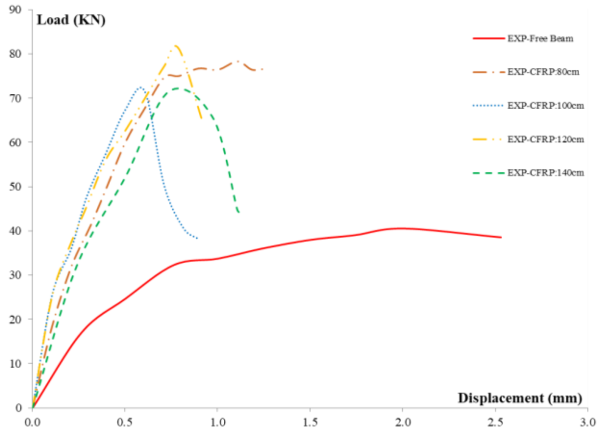

Figure 15: Comparison of load-displacement diagram of CFRP beams

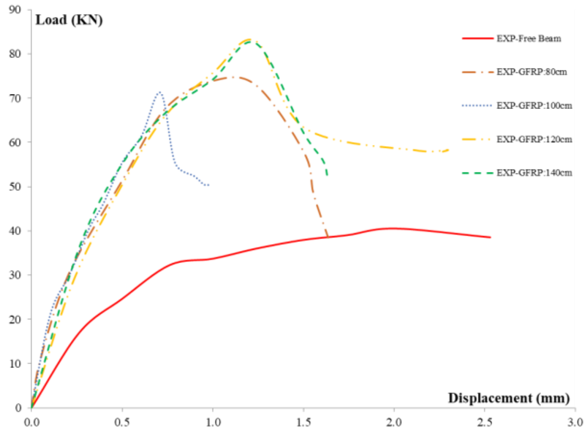

Figure 16: Comparison of load-displacement diagram of GFRP Beams

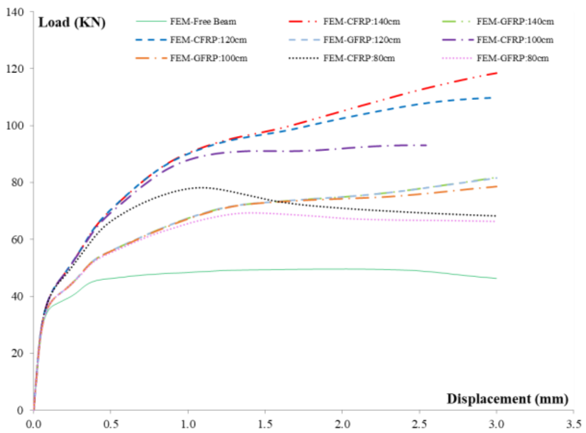

Figure 17: Load-displacement diagram of beams with CFRP and GFRP reinforcement (numerical method)

JOMAse | Received: 02-December-2023 | Accepted: 30-March-2024 | [(68) 1: 1-8]
Published by International Society of Ocean, Mechanical and Aerospace Scientists and Engineers, www.isomase.org., ISSN: 2354-7065 & e-ISSN: 2527-6085

ISOMAse International Society of Ocean, Mechanical and Aerospace Scientists and Engineers
Journal of Ocean, Mechanical and Aerospace
-Science and Engineering-
30th March 2024. Vol.68 No.1

Table 7: Results of the manufactured beams in the laboratory and modeled in ABAQUS® Software

Sample Number	Displacement (mm)	Experimental Ultimate Strength (KN)	Theoretical Ultimate Strength (KN)	Increase in Experimental Ultimate Strength Compared to Unstrengthen State (%)	Increase in Theoretical Ultimate Strength Compared to Unstrengthen State (%)	Increase/Decrease in Displacement at Ultimate Strength Compared to Unstrengthen State (%)	Failure Location	Failure Mode
B0	12.53	57.07	48.37	0.00	0.00	0.00	The midspan region of the beam	Crushing of the compressive concrete
B1	8.79	63.07	77.91	10.51	61.07	-29.85	The midspan region of the beam	Shear failure
B2	7.41	66.78	88.00	17.01	81.93	-40.86	The midspan region of the beam	Premature failure (peeling of the concrete cover)
B3	8.87	77.01	89.93	34.94	85.92	-29.21	The midspan region of the beam	Shear failure
B4	8.27	88.75	90.57	55.51	87.24	-34.00	The midspan region of the beam	Premature failure (crushing of the compressive concrete)
B5	9.6	59.98	65.60	5.10	35.62	-23.38	The midspan region of the beam	Shear failure
B6	9.76	61.80	67.25	8.29	39.03	-22.11	The midspan region of the beam	Premature failure (shear failure)
B7	9.66	71.81	68.13	25.83	40.85	-22.90	The midspan region of the beam	Premature failure
B8	9.24	82.06	69.35	43.79	43.37	-26.26	The midspan region of the beam	Premature failure (shear failure)

Table 8: Economic results of samples

Sample Number	Ultimate Strength Laboratory (KN)	CFRP Sheet Consumption (M^2)	GFRP Sheet Consumption (M^2)	Total Reinforcement Cost per Square Meter (US$)
B_1	63.07	0.24	---	18.8
B_2	66.78	0.30	---	21.8
B_3	77.01	0.36	---	24.6
B_4	88.75	0.42	---	28.2
B_5	59.98	---	0.24	16.4
B_6	61.80	---	0.30	18.8
B_7	71.81	---	0.36	21
B_8	82.06	---	0.42	23.6

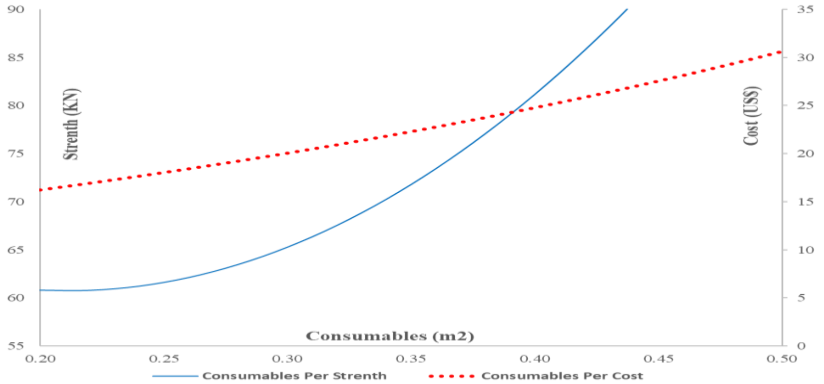

Figure 18: Resistance-cost-materials consumption chart

JOMAse | Received: 02-December-2023 | Accepted: 30-March-2024 | [(68) 1: 1-8]
Published by International Society of Ocean, Mechanical and Aerospace Scientists and Engineers, www.isomase.org., ISSN: 2354-7065 & e-ISSN: 2527-6085

5.0 CONCLUSION

The use of FRP sheets for the strengthening and rehabilitation of reinforced concrete structures is increasing day by day due to its numerous and well-known advantages. The necessity of retrofitting and seismic design of structures and understanding their performance against earthquakes, especially in a country like Iran located in a seismically active zone, is a top priority. Therefore, further research on FRP strengthening methods, both theoretically and experimentally, is essential. It was observed that with an increase in the length of FRP sheets, the resistance of reinforced concrete beams compared to the reference concrete beam increased by approximately 61%, 82%, 86%, and 87%, respectively. The use of FRP sheets enhances the flexural capacity of beams, and the tensile-to-strain ratio of FRP sheets remains generally constant and does not change. If the designer determines that the design environment is not aggressive or takes preventive measures against environmental degradation using protective coatings, the experimentally obtained durability factors can be used to modify the code factors. The crucial point in this regard is to ensure that the protective coating does not deteriorate during the structure's lifespan, and durability tests should be performed. One of the disadvantages of FRP sheets is early failure, preventing the cross-section from reaching its flexural capacity after strengthening. Since the design of concrete sections for FRP strengthening is based on the required compressive strength, the length of FRP strengthening sheets can be optimized to reduce the cost of FRP sheets and use them efficiently, thus reducing costs.

REFERENCES

[1] American Concrete Institute Technical Committee 440, (2008). Guide for the design and construction of externally bonded FRP systems for strengthening concrete structures, ACI 440.2R-08.

[2] Klamer, E.L., Hordijk, D.A. & Hermes, M.C.J. (2008). The influence of temperature on RC beams strengthened with externally bonded CFRP reinforcement. *Heron*, 53(3), 157-186.

[3] Tuakta, C. & Buyukozturk, O. (2011). Deterioration of FRP/concrete bond system under variable moisture conditions quantified by fracture mechanic, *Composite Part B: Engineering*, 42(2), 145-154.

[4] Nanni, A. (1995). Concrete Repair with externally bonded FRP reinforcement. *Concrete International*, 17(6), 22-26.

[5] Nanni, A., Focacci, A. & Codd. C.A. (1998). Proposed procedure for the design of RC flexural members strengthened with FRP sheets. *Second International Conference on Composites in Infrastructure*, Tucson, Arizona, USA,1, 187- 201.

[6] Nanni. A. & Gold. W. (1998). Strength assessment of external FRP reinforcement, *Concrete International*, 20(6), 39- 42.

[7] Mostofinejad, D. & Hajrasouliha, M.J. (2009). Investigating the influencing factors on the performance of the grooving method in controlling the separation of the FRP sheet from the concrete surface. The *5th national construction congress*, Mashhad, Iran.

[8] Mostofinejad, D. & Mahmoudabadi, E. (2010). Grooving as alternative method of surface preparation to postpone debonding of FRP laminates in concrete beams. *Journal of Composites for Construction*,14(6), 804-811.

[9] Mostofinejad, D. & Shameli, M. (2010). Performance of EBROG method under Multilayer FRP sheets for flexural strengthening of concrete beans. *The 12th East Asia-Pacific Conference on Structural Engineering and Construction (EASEC-12)*, Hong Kong, China.

[10] Sadremomtaz, A. & Rostami-Atigh, H. (2012). Investigating the effect of the CFRP sheet end connection method on the failure mode of reinforced concrete beams in bending. *The 4th Annual National Concrete Conference of Iran*, Tehran, Iran.

[11] Varastehpour, H. & Eskenati, A.R. (2015). Increasing the bending capacity of reinforced concrete beams using glass composite fibers. The *7th Annual National Concrete Conference of Iran*, Quarchak, Iran.

[12] Varastehpour, H. & Kermani, F. (2015). A new method of reinforcing concrete beams using carbon fibers. *The 7th Annual National Concrete Conference of Iran*, Quarchak, Iran.

[13] Mostofinejad, D. & Hajrasouliha, M.J. (2009). Experimental evaluation of effective restraint length of FRP reinforcement sheets on concrete surface. *The 10th International Congress of Civil Engineering*, Tabriz, Iran.

[14] Sajjadi-Manizani, B., Tavousi-Tafreshi, Sh. & Akbarpour, A. (2015). The Comparison between Using Multilayers of High Resistance GFRP on Ductility with Multilayers of High Resistance CFRP. *The 7th International Conference of Seismology and Earthquake Engineering*, Iran.

[15] American Concrete Institute, (2005). Building code requirements for structural concrete and commentary, ACI 318M-05.

[16] American Concrete Institute Technical Committee 440, (2002). Guide for the design and construction of externally bonded FRP systems for strengthening concrete structures, ACI 440.2R-02.

JOMAse | Received: 02-December-2023 | Accepted: 30-March-2024 | [(68) 1: 1-8]
Published by International Society of Ocean, Mechanical and Aerospace Scientists and Engineers, www.isomase.org., ISSN: 2354-7065 & e-ISSN: 2527-6085